Continuum model of voltage-dependent gating

Macroscopic conductance, gating current, and single-channel behavior

David G. Levitt
Department of Physiology, University of Minnesota, Minneapolis, Minnesota 55455

ABSTRACT It is assumed that the conformational change of the voltage-gated channel is continuous, characterized by movement along a generalized one-dimensional reaction coordinate, x, varying from 0 to 1. This large conformational change is coupled to the movement of most of the gating charge. Superimposed on this large movement is a smaller, very fast conformational change that opens or closes the channel. The large conformational change perturbs the channel so that opening is favored near $x = 1$ and closing is favored near $x = 0$. The movement along the x axis is described by a generalized Nernst-Planck equation, whereas the open-close transition is modeled as a discrete reaction-rate process. The macroscopic conductance, gating current, and single-channel behavior of a simple, linearized version of the model is described. Although the model has only seven adjustable constants (about the same as would be required for a conventional three-state model), it can mimic the behavior of the delayed rectified K^+ channel with 12 or more closed states. The single-channel behavior of the model can have bursts of rapid openings and closings, separated by long closed times. If the conformational change is assumed to correspond to the rotation and translation of charged helices, then this model can be used to estimate the effective rotational diffusion coefficient of the helix. Such calculations for the delayed rectifier K^+ channel indicate that the motion must be very restricted.

INTRODUCTION

The conventional approach to modeling the gating of ion channels is based on the use of state diagrams, each state representing a different conformation of the channel protein (Hille, 1984). This is a very robust model, with enough flexibility and adjustable parameters to describe any conceivable set of kinetics. For voltage-sensitive channels, the model is usually reduced to a series of closed states leading to one open state (and, possibly, an inactivated state) with voltage-dependent transitions between the states. One difficulty with this model is that, for many channels, a large number of closed states are required to explain the time delay between depolarization and channel opening. The most extreme example is the squid delayed rectifier K^+ channel, which requires as many as 25 closed states (Cole and Moore, 1960). This presents a conceptual problem because such a large number of discrete conformations does not seem physically realistic. This problem could be avoided in a natural way if it was assumed that the channel could be described by a continuum of states. The purpose of this paper is to develop a general continuum model of channel gating that can provide an alternative to the conventional model.

The continuum model that will be described here is actually a generalization of the discrete model and, therefore, with the appropriate choice of parameters, can describe any set of kinetics that can be described by the discrete model. Thus, unfortunately, it is not possible to use experimental data to discriminate between the models. However, the continuum approach has several useful properties. (*a*) If there are a large number of states, the continuum description is simpler, replacing a long listing of seemingly arbitrary rate constants by two energy profiles (and two kinetic constants). These energy plots provide an immediate global picture of the gating behavior of the channel. (*b*) The continuum model is a more physically realistic description. For example, recent sequence analysis suggests that voltage-dependent gating involves the rotation and translation of specific helical segments (Salkoff et al., 1987). The continuum model provides a description in terms of the energy profile that this segment experiences during its rotation and the effective rotational diffusion coefficient of this segment. Recently, several models of gating have been proposed that have fractal type kinetics (Liebovitch and Sullivan, 1987; Läuger, 1988; Millhauser et al., 1988). In contrast to these more radical models, the model proposed here represents only a slight extension and generalization of the conventional model.

The general features of the continuum model will be illustrated by looking at the results of a greatly simplified version in which the general functions are replaced by simple linear relations. The macroscopic conductance, gating current, and single-channel properties will be described for two versions. The simple model is characterized by seven constants. This is no more than what would be required to describe the rate constants and voltage

0006-3495/89/03/489/10 $2.00

dependence for three discrete states. And yet, as will be shown, the behavior of this simple model is very rich in detail, mimicking channels that have from 1 to 12 (or more) open or closed states.

DESCRIPTION OF MODEL

The first issue that must be faced in developing a continuum model is the evidence that the transitions between the different conductance states is discrete. Although the physical opening of the channel has to be continuous, it must occur on a time scale that is much faster than the limits of resolution of the best preparations: ~10 μs (Colquhoun and Sakmann, 1981). This is in marked contrast to the slow process that precedes opening. In the squid axon, opening of the K^+ channel can be delayed by as much as 0.5 ms after the depolarization. A similar but less dramatic delay is seen for the squid Na^+ channel (Taylor and Bezanilla, 1983). Gating current measurements on the Na^+ and K^+ channels indicate that during this delay there is movement of gating charge which is associated with slow changes in protein conformation (Taylor and Bezanilla, 1983; White and Bezanilla, 1985). This suggests that there are two separate processes involved in gating: a slow (presumably large) conformational change during which most of the gating charge moves, and a fast (presumably small) conformational change which opens the channel.

The model shown in Fig. 1 incorporates this idea of two separate time scales. The slow large conformational change is represented by continuous movement along the horizontal x axis, where x is a generalized reaction coordinate. The fast open-close transition is represented by jumps between the lower (closed) and upper (open) states. The fast and slow conformational changes are assumed to be separate events, and, therefore, the channel can potentially open or close at any value of x. However, the probability of opening (k_o) or closing (k_c) is a function of x and the parameters will be chosen so that the channel has a significant probability of opening only when the channel is near the far end ($x = 1$).

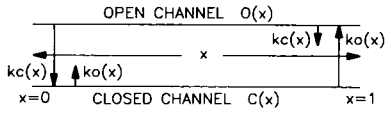

FIGURE 1 Diagram of continuum model. Horizontal lines depict the continuum of open (*upper*) and closed (*lower*) states, where x is a general reaction coordinate. The channel protein conformation drifts along the x axis under the influence of the applied voltage. The transition between the closed and open states is discrete and can occur at any value of x. The rate of this discrete transition is determined by the rate constant $k_o(x)$ (opening) and $k_c(x)$ (closing).

Physically, one can imagine that the continuous movement corresponds to the rotation and translation of a charged helix (or helices), with x proportional to the angle of rotation. The opening or closing of the channel involves a different conformational change on a separate part of the protein. When x is near zero, the closed form has a lower energy and, therefore, is the more probable state. The rotation of the helix towards $x = 1$ produces a distortion in the protein, lowering the energy of the open state relative to the closed state, so that the open state becomes more probable. It will be assumed that movement along x is directly associated with movement of the gating charge in the applied potential field. Thus, changes in membrane potential will drive movement along the x axis, opening or closing the channel.

EQUILIBRIUM BEHAVIOR

The above qualitative discussion emphasizes that the behavior of the channel depends on the probability that the channel is open or closed as a function of the reaction coordinate x. Quantitatively, this probability is related to the energy of the open ($uo(x)$) and closed channel ($uc(x)$) as a function of x (the energy will be expressed in units of kT so that the functions are dimensionless). It will be assumed that these two functions have a linear dependence on x and can be written as:

$$\begin{aligned} uc(x) &= A(1 - x) + uv(x) \\ uo(x) &= uc(x) + uoc(x) \\ uv(x) &= n_g(1 - x)v \\ uoc(x) &= C(1 - x - B) - n_o v. \end{aligned} \tag{1}$$

The function $uoc(x)$ is the energy difference between the open and closed state. The applied membrane potential, v (in units of $kT/e = 25$ mV) influences the energy in two ways. First, it is assumed that as x varies from 0 to 1, an "equivalent" gating charge n_g (=3 in the following calculations) moves across the membrane, contributing the term $uv(x)$ to the energy of the closed and open states. Second, during the fast transition from the closed to open state, an additional smaller charge n_o (=1) moves across the membrane. The energy functions are characterized by five constants: A, B, C, n_g, and n_o.

The results for two sets of constants will be described. For both models it is assumed that the total gating charge is 4, with $n_g = 3$ and $n_o = 1$. In "Model 1" the parameters were chosen so that the channel could open only when x was close to 1. This choice requires maximum movement of the gating charge before the channels can open. The potential functions for Model 1 are shown in Fig. 2 at three different values of the applied voltage (v).

The general behavior of the channel can be understood

simply from the energy profiles shown in Fig. 2. The equilibrium probability that the channel is in the closed (C) or open (O) state at position x is given by:

$$C(x) = \frac{1}{Q} e^{-uc(x)}$$

$$O(x) = \frac{1}{Q} e^{-uo(x)}$$

$$Q = \int_0^1 (e^{-uc(x)} + e^{-uo(x)})\, dx. \qquad (2)$$

Channel opening is favored for values of x where $uo(x) < uc(x)$ corresponding to values of $uoc(x)$ $(=uo - uc)$ that are <0. In Model 1, the parameters B and C are chosen so that uoc has a steep dependence on x and, at $v = 0$, $uo < uc$ only for the last 5% of the reaction coordinate.

The total probability that the channel is open or closed is equal to the integral of the probability over x. Fig. 3 shows a plot of the equilibrium fraction of channels that are open as a function of voltage. The constants in the energy functions were chosen so that this curve would be similar to that observed experimentally for the squid K^+ conductance. At a voltage of -20 mV, the channel has about a 50% chance of being open. At this voltage, $uc(x)$ is nearly constant (Fig. 2, *middle*), so that the closed channels will be roughly evenly distributed along x, whereas most of the open channels will be in the region $x > 0.95$. At $v = +100$ mV, almost all the channels are open and concentrated in the region $x > 0.9$ where $uo < uc$ (Fig. 2, *top*). At $v = -100$ mV, the channels are nearly 100% closed and most of the channels will have values of x near $x = 0$, where uc is a minimum (Fig. 2, *bottom*).

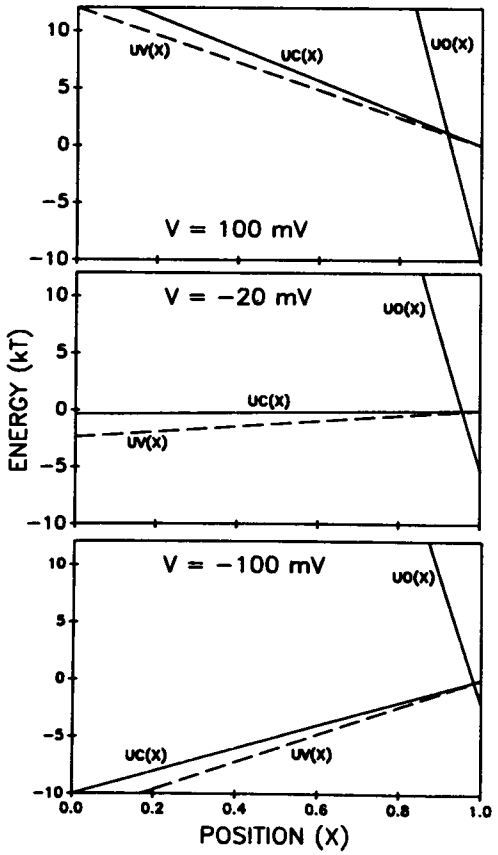

FIGURE 2 Energy diagram for Model 1. Curves show the energy as a function of the reaction coordinate (x) at different values of the applied voltage (V). uc is the energy of the closed state, uo the energy of the open state, and uv the energy associated with the applied voltage. At a V of -20 mV, the channels are ~50% open. Constants in Eq. 1 are $A = 2$, $B = 0.05$, $C = 120$, $n_g = 3$, and $n_o = 1$.

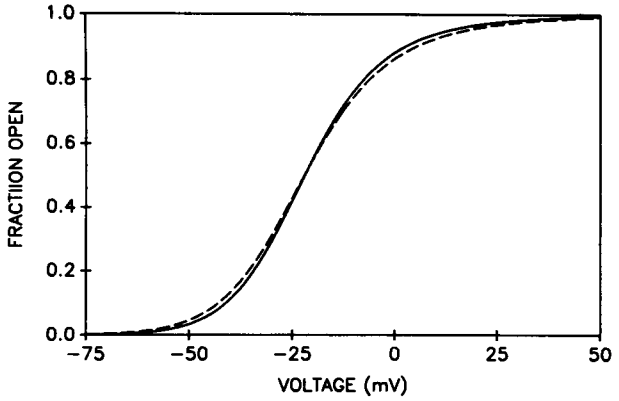

FIGURE 3 Equilibrium fraction of open channels as a function of membrane potential: Model 1 (——); Model 2 (– – –).

Consider now what happens if channels which are at equilibrium at -100 mV are suddenly depolarized to $+100$ mV. The potential energy of the channels is instantaneously shifted from the bottom to the top panel in Fig. 2. However, the channels cannot open until they are in a region where $uo(x) < uc(x)$, i.e., at x close to 1. The closed channels will drift through conformations under the influence of the applied voltage until they reach values of x near 1, and then they will open. This drift time leads to a delay in channel opening. In contrast, if the membrane is originally at a potential of $+100$ mV and suddenly hyperpolarized to -100 mV, uo is greater than uc for nearly all the channels which, therefore, can immediately close without any time delay.

Fig. 4 shows the second, contrasting, set of energy profiles used for "Model 2." The only difference is in the constants B and C used to describe uoc (the energy difference between the open and closed state). The constant B is equal to 0.3 which means that (at $v = 0$) the open form of the channel is favored over the last 30% of x. The constant C was chosen so that the voltage at which the channels were 50% open would be similar to Model 1.

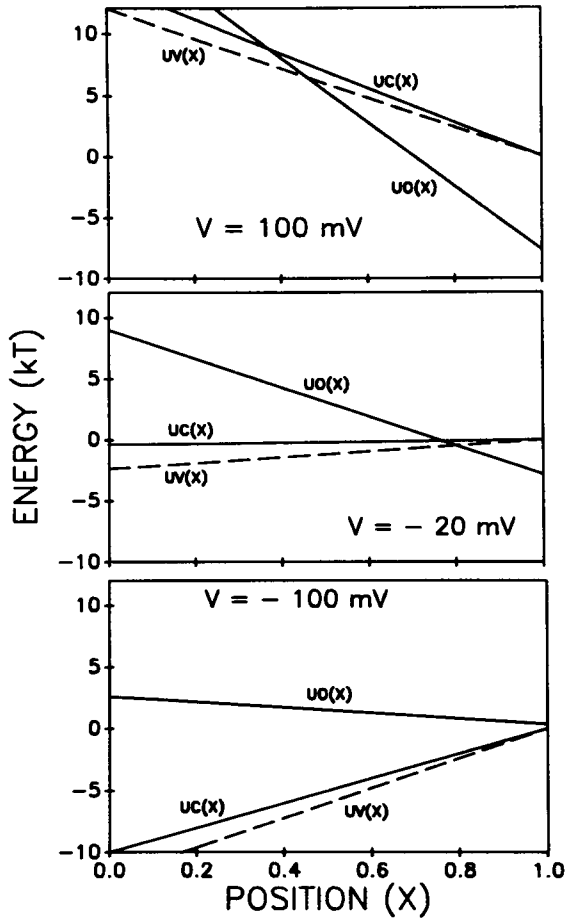

FIGURE 4 Energy diagram for Model 2. The constants are the same as for Model 1 (Fig. 2) except that $B = 0.3$ and $C = 12.26$.

The dashed curve in Fig. 3 shows that the voltage dependence of the probability a channel is open is similar for the two models. This indicates that both models would have similar steady-state conductance vs. voltage behavior. However, from an examination of potential curves in Figs. 2 and 4, it is apparent that the behavior of Model 2 should be significantly different from that of Model 1 when it is suddenly depolarized from −100 to +100 mV. As can be seen from the top panel in Fig. 4, $uc > uo$ for all values of $x > 0.4$, and thus the channels can open after only drifting a short distance, corresponding to a short time delay.

MACROSCOPIC CONDUCTANCE AND GATING CURRENT

The above discussion is only qualitative. To obtain quantitative results, a detailed kinetic model must be used. It will be assumed that the continuum movement of the channel along the reaction coordinate (x) can be described by a generalized Nernst-Planck equation with a generalized mobility (diffusion coefficient) $D(x)$ and the transition from the closed to open (or open to closed) state is characterized by a rate constant $k_o(x)$ (or $k_c(x)$). The general time-dependent case is then described by the following set of coupled partial differential equations.

$$\frac{\partial C}{\partial t} = -\frac{\partial J_c}{\partial x} + k_c O - k_o C$$

$$\frac{\partial O}{\partial t} = -\frac{\partial J_o}{\partial x} + k_o C - k_c O$$

$$J_c = -D_c(x)\left(\frac{\partial C}{\partial x} + C\frac{duc}{dx}\right)$$

$$J_o = -D_o(x)\left(\frac{\partial O}{\partial x} + O\frac{duo}{dx}\right), \qquad (3)$$

where J_c and J_o are the flux along the closed and open states and $C(x)$ and $O(x)$ are the probability the channel is in the closed and open state at position x (boundary condition: $J_c = J_o = 0$ at $x = 0$ and $x = 1$). The system must satisfy the microscopic reversibility condition which means that at every x, the equilibrium probability of opening and closing must be equal. This implies that

$$k_c(x) = k_o(x)e^{-uoc(x)}. \qquad (4)$$

Thus, in general, the system is described by five functions: $D_c(x)$, $D_o(x)$, $k_o(x)$, $uc(x)$, and $uoc(x)$. With this number of adjustable functions, most sets of experimental kinetics could be satisfied. In the examples used to illustrate the model, the following simplifying assumptions are made:

$$D_c(x) = D_o(x) = D$$

$$k_o(x) = ke^{-1/2uoc(x)}, \qquad (5)$$

where D and k are constants. The constant D can be eliminated by defining a dimensionless time $\tau = Dt$ (the spatial units of D are in the dimensionless units of x). Thus, this system is completely described by the two energy functions (uc and uo) described in the Equilibrium Behavior section and the one parameter k. A k of 100 was used for all the calculations in this paper. This relatively large value was chosen so that transitions between open and closed states would be fast compared with movement along the x axis. This emphasizes the continuum features of the model. It is consistent with the experimental measurements on the squid K^+ channel which indicate that the step that involves the physical opening of the channel is not rate limiting (White and Bezanilla, 1985). Details of the numerical solution are described in the Appendix.

Fig. 5 shows the equilibrium probability that an opening or closing will occur at different values of the reaction coordinate x (for $v = -20$ mV). This rate is equal to the opening rate (k_0) at x times the equilibrium probability the channel is closed at x. It can be seen that for Model 1 the channel will open or close only for values of x very close to 1. In contrast, for Model 2, a significant number of transitions occur over the last 50% of the reaction coordinate x.

The time course of the macroscopic conductance was found by first preparing the system at equilibrium at some initial voltage and then, suddenly, switching to a final voltage and solving for the time-dependent change in the number of open and closed channels. Figs. 6 and 7 show the time course of the change in the fraction of open channels, first, for channel opening when the voltage is jumped from -150 to $+100$ mV, and then for channel closing when the voltage is returned to -150 mV. In agreement with the above qualitative discussion, there is a delay in opening (Fig. 6) when the channels are depolarized to $+100$ mV and no delay in closing when the channels are hyperpolarized back to -150 mV.

Because the macroscopic conductance should be proportional to the fraction of open channels, the curves in Figs. 6 and 7 can be directly compared with experimental conductance measurements. The time axis was scaled by choosing $D = 100\ s^{-1}$ so that the delay in channel opening in Fig. 6 was approximately the same as for the squid axon K^+ conductance. This scaling is used in all subsequent calculations. The shape of this conductance change is remarkably similar to that observed for the squid K^+ conductance, especially because the parameters were not adjusted to get this result. The closed circles are the fit to the data using the functional form originally proposed by Hodgkin and Huxley (1952): $[1 - \exp(-t/\tau_n)]^n$ for opening and $\exp(-mt/\tau_n)$ for closing. Although Hodgkin and Huxley used an $n = m = 4$ for both closing and

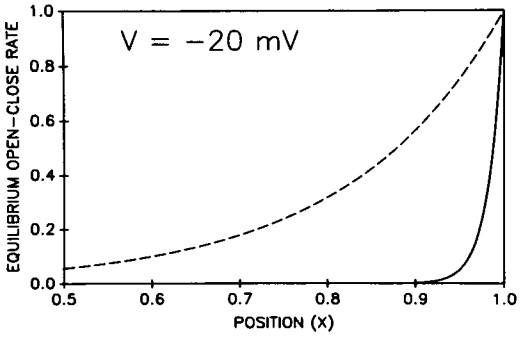

FIGURE 5 Equilibrium probability that a transition (opening or closing) will occur as a function of the reaction coordinate (x) for Model 1 (——) and Model 2 (---) at a voltage of -20 mV.

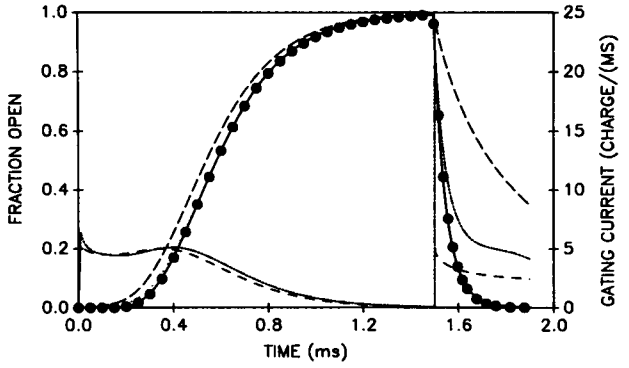

FIGURE 6 Model 1 time dependence of gating current and the probability a channel is open during a transient change in membrane potential. At time zero, the channel, which is at equilibrium at either -150 mV (——) or -75 mV (---), is depolarized to $+100$ mV and the fraction of channels that are open is plotted as a function time. After the channels have equilibrated at $+100$ mV the membrane is hyperpolarized back to -150 or -75 mV and the closing of the channels is shown. The opening curve for the initial potential of -75 mV can be made to superimpose quite closely on the -150 mV curve by a time shift (···). The curve can be fit (●) by an equation of the form of $[1 - \exp(-t/\tau_n)]^n$ for opening and $\exp(mt/\tau_n)$ for closing with $\tau_n = 0.201$ ms, $n = 12$, and $m = 6$. Also shown is the corresponding gating current (in units of electron charge per millisecond) for an initial voltage of -150 mV (·—·) and -75 mV (---).

opening, Cole and Moore (1960) showed that the n for opening depended on the degree of initial hyperpolarization and could reach values as large as 25. For the curve in Fig. 6, n is 12 and m (the closing value of n) is ~6, similar to the results of Cole and Moore. Presumably, by fiddling with the parameters it should be possible to get even longer delays and larger values of n.

The corresponding result for an initial potential of -75 mV (depolarized again to $+100$ mV) is also shown in Fig.

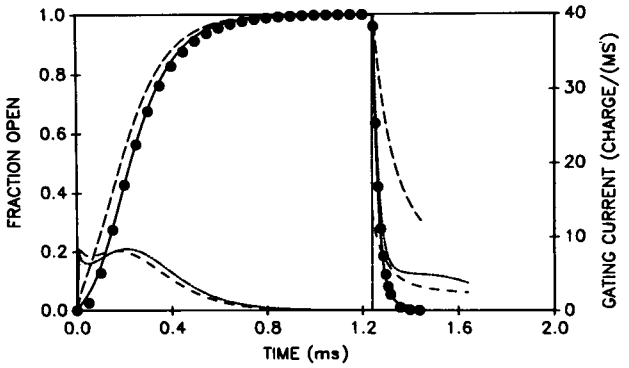

FIGURE 7 Model 2 time dependence of gating current and the probability a channel is open during a transient change in membrane potential. See legend to Fig. 6. Constants used in exponential fit were $\tau_n = 0.142$ ms, $n = 3$, and $m = 6$.

6. The time course of channel opening is shifted to the left, similar to what is observed experimentally. The subsequent closing of the channel is markedly slower at this value of the resting potential because the removal of the newly closed channels from the $x = 1$ region by diffusion has now become rate limiting. The closing rate is very sensitive to the value of k while the opening rate is relatively independent of k as long as it is large enough. Fig. 7 shows a similar set of curves for Model 2. As was predicted qualitatively from the equilibrium behavior, the time delay is much less marked because channels can open over most of the length of the reaction coordinate.

Also shown in Figs. 6 and 7 is the time course of the gating current (see Appendix for details). For a depolarizing potential, there is a large gating current during the time period that corresponds to the time delay in channel opening. This results from the movement of the charge n_g (=3) associated with the drift in channel conformation toward the region where opening can occur ($x = 1$). There is a second bump in gating current at the time of channel opening associated with the movement of the charge n_0 (=1), the charge that moves through the entire voltage field during a close-open transition. When the membrane is hyperpolarized and the channels rapidly close, there is a burst of gating current associated with the charge n_0 and a slower, prolonged current associated with the drift of the charge n_g. The time constant of this fast component of closing gating current is similar to the macroscopic conductance time constant, as is observed experimentally for the squid Na^+ and K^+ channel. The corresponding gating current for an initial depolarization of -75 mV is smaller and time shifted relative to the current for a depolarization of -150 mV.

SINGLE-CHANNEL PROPERTIES

The ability to measure the time sequence of the opening and closing of a single channel provides information about the underlying channel kinetics that is of much higher resolution than can be obtained from macroscopic measurements. In this section the single channel features of the simple continuum model will be described.

The simplest type of analysis is the measurement of open or closed time histograms or frequencies. If there is only one open (or closed) state then the open (or closed) time frequency should be a single exponential. Ideally, the number of exponentials is equal to the number of states. For many voltage sensitive channels the data indicates that there is only one open state and a number of closed states. For the continuum model, the open channel theoretically consists of an infinite number of states corresponding to the different values of x. However, if the range of x that the open channel can occupy is small, and diffusion is fast enough to average over all the values of x before the channel closes, then it could behave kinetically as if it were a single state. It will be shown that Model 1 satisfies these conditions.

When the channel opens from the closed state $C(x_0)$, $O(x)$ will be initially infinite at x_0 and zero everywhere else (a delta function). Using this initial condition, the open time frequency can be obtained by solving for the time course of closing of the channel, for the case where no back transitions from the closed to open state are allowed (closed state is absorbing). The fraction of channels that close in each time interval will be defined as the "open time frequency" and the integral of this function is the "cumulative open time." The open time frequency is the probability that the open channel closes during a time interval dt about the point t. The cumulative open time is equal to the fraction of channels that are closed after a time t. These two functions for Model 1 are plotted in Fig. 8 for two different values of x_0 (the value of the reaction coordinate at which the channel initially opens). The value of $x_0 = 0.97$ is at the very lower limit of the probable open region for Model 1 and channels would rarely open into this position (see Fig. 5), whereas $x_0 = 0.99$ is in a region where a large fraction of the openings should occur. These solutions are for a voltage (v) of -20 mV, chosen because there should be equal numbers of open and closed channels in the steady state. The cumulative open time curve is nearly identical for the two positions, providing direct evidence that the open condition for this model behaves kinetically like a single state. This is also supported by the fact that the curve can be fitted by a single exponential (*solid circles*). Paradoxically, the open time frequency (normalized so that the maximum value is

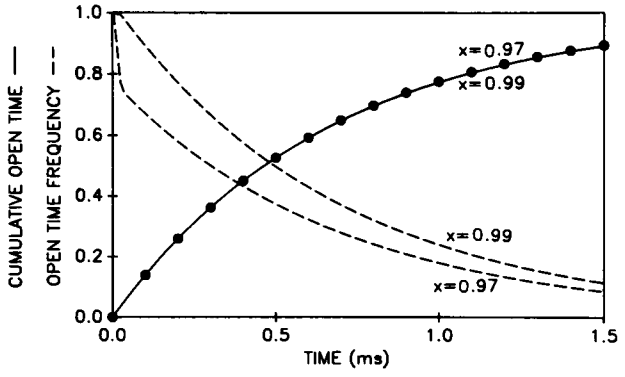

FIGURE 8 Model 1 cumulative open time (——) and open time frequency (– – –) at a potential of -20 mV. Results are shown for two different values (0.99 and 0.97) of the position (x_0) where the initial opening occurs. The open time frequency is arbitrarily scaled so that the maximum rate = 1. The cumulative open time curves for the two positions cannot be distinguished. The cumulative open time is fit (●) by a single exponential: $1 - \exp(-1.5t)$.

1) is not identical for the two values of x. This is because the channel that opens at $x_o = 0.97$ is in a relatively unstable state, having an energy *uo* very close to that of the closed state *uc* (see Fig. 2, *middle*), and will tend to close more rapidly than average. However, because it quickly diffuses out of this region toward larger values of x, the relatively high rate of closing occurs for only a very short time (~0.05 ms) and not enough channels close to significantly change the cumulative function. Because these channels would have an open lifetime of <0.05 ms, they probably could not be detected experimentally. Thus, from just a measurement of open times it would not be possible to distinguish this continuum model from a model with one open state.

The closed time frequency and cumulative closed time for Model 1 at the same voltage (20 mV) and values of x_o (0.97 and 0.99) is shown in Fig. 9 for a time scale of 0 to 0.5 and 0 to 5 ms (*inset*). The cumulative curve is characterized by an extremely wide range of time scales. Two exponentials (*solid circles*) are required to fit the short lifetimes (<0.1 ms) but four or more exponentials would be needed to fit the entire curve. Physically, these results are predictable from an examination of the energy curves in Fig. 2. Because the open region occupies such a small fraction of the total reaction coordinate, opening must be highly favored in this region. This means that most channels that close will quickly reopen. However, occasionally, a channel will manage to drift out of this region before reopening. Once this occurs, it will have a very low probability of opening because, in most of the coordinate space, the closed form is much more probable. This wide range of time scales and high frequency of short closings is a characteristic feature of the closed time distribution of the continuum model. It is also the outstanding experimental feature for most ion channels,

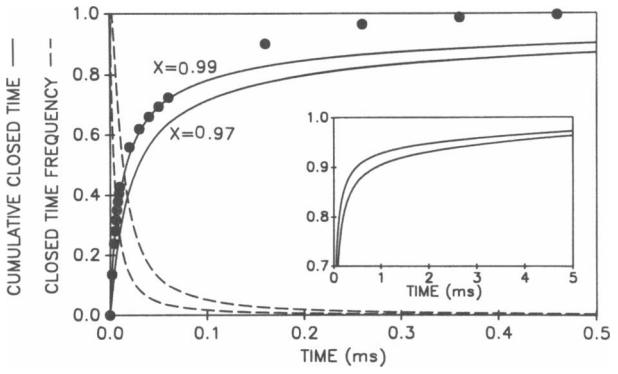

FIGURE 9 Model 1 cumulative closed time (——) and closed time frequency (---) at a voltage of −20 mV for $x_o = 0.99$ and 0.97. Two exponentials (●) can fit only the early part of the curve: $1 - 0.49 \exp(-146t) - 0.51 \exp(-10.2t)$. Inset shows the long time behavior.

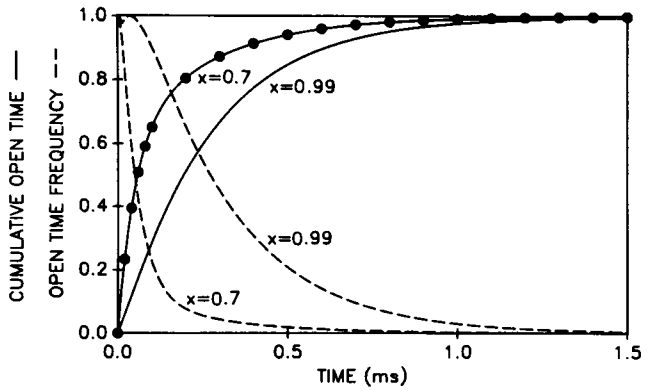

FIGURE 10 Model 2 cumulative open time (——) and open time frequency (---) at a potential of −20 mV. See legend, Fig. 8. The curve for $x_o = 0.7$ can be fit (●) by the two exponential equation: $1 - 0.59 \exp(-20.8t) - 0.41 \exp(-3.89t)$.

and lends some support, although indirect, to this type of model.

The experimentally measured closed time distribution will differ markedly from the theoretical curve in Fig. 9 because the response time of the recording apparatus is too slow to detect the short closings. For example, if closings <0.1 ms were not detected, only the last 20% of closings would be seen and one would conclude that the closed lifetime was several milliseconds (see inset).

Figs. 10 and 11 show the open and closed time calculations for Model 2. For this model, the cumulative open time (Fig. 10) depends on x_o, the position the channel was in when it opened. To obtain the experimental open time it would be necessary to determine the average of such curves for all values of x, weighted by the equilibrium

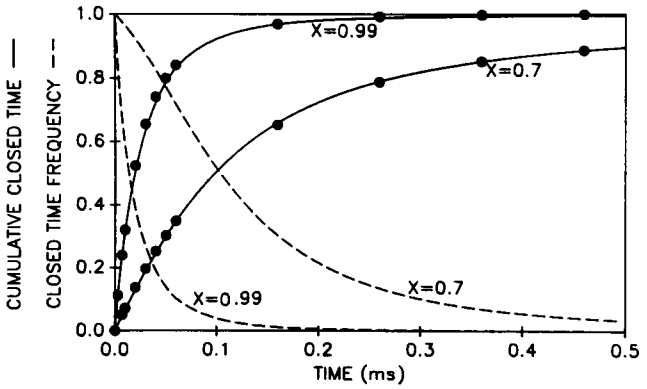

FIGURE 11 Model 2 cumulative closed time (——) and closed time frequency (---) at a voltage of −20 mV for $x_o = 0.99$ and 0.7. See legend, Fig. 9. The curves could be fit (●) by two exponentials: $x_o = 0.99$, $1 - 0.7 \exp(-50.9t) - 0.3 \exp(-14.3t)$; $x_o = 0.7$, $1 - 0.82 \exp(-8.76t) - 0.18 \exp(-1.29t)$.

probability the channel opened at x. Because the cumulative open time for each x_0 can be fitted by two exponentials (*solid circles*), the open condition for this continuum model would behave kinetically as if it consisted of two discrete states. The closed time functions for Model 2 (Fig. 11) can also be fit by two exponentials and thus do not have the wide variation in time scales that characterized Model 1. This could be predicted from the energy curves (Fig. 4) because the channel in Model 2 can open over a wider range of the reaction coordinate.

The single channel behavior of these models can be more easily visualized by simulating the random behavior of a channel using the Brownian dynamics approach (Cooper et al., 1985) to model the movement along the x axis and a random function to determine when an open-close transition occurs (see Appendix). The simulated results are shown in Fig. 12 (Model 1) and Fig. 13 (Model 2). Although it appears as if the open state probability in Fig. 13 is much higher than in Fig. 12, this is misleading, because the open probability is similar in the two figures (0.44 in Fig. 12 and 0.53 in Fig. 13). In Fig. 13, a significant amount of closed time is obscured in the open "bursts." The simulated data for Model 1 highlights the wide variation in time scales that was evident in the closed time functions, with bursts of very rapid openings and closings separated by closed times of up to 10 ms.

One would predict that for Model 2 the adjacent open and closed intervals should be correlated. For example, suppose the channel opens from position $x = 0.5$ at a voltage of -20 mV (see Fig. 4, *middle*). Because the open channel has a higher energy than the closed channel, it should have a high rate of closing and, consequently, a short open time. In contrast, the closed state at $x = 0.5$ will have a low rate of opening and therefore a long closed time. The opposite relation would be predicted for openings and closings at, e.g., $x = 0.9$. Thus, one would predict that closed times should be inversely correlated with the length of adjacent open times. Just such an effect was experimentally observed by McManus et al. (1985) for a Cl^- channel and for a Ca^{2+} activated K^+ channel. They interpreted this observation in terms of a discrete state analogue to the continuum Model 2. The ease with which this type of correlation can be predicted just by an examination of the energy diagram provides an illustration of the advantage of the continuum model.

A calculation similar to that of McManus et al. (1985) was performed on the simulated continuum single channel data. In a run of 10,000 open-close transitions, closed times were grouped into discrete intervals and the average

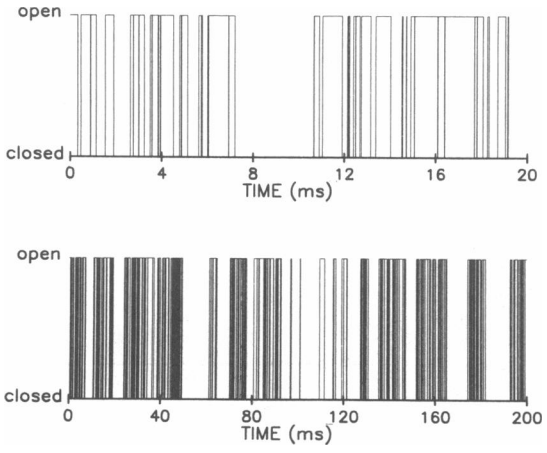

FIGURE 12 Simulated single channel behavior of Model 1. The opening and closing at $V = -20$ mV for a period of 200 ms is shown in the bottom panel. Top panel shows the first 20 ms of this record. Average fraction open = 0.44; 459 open-close transitions.

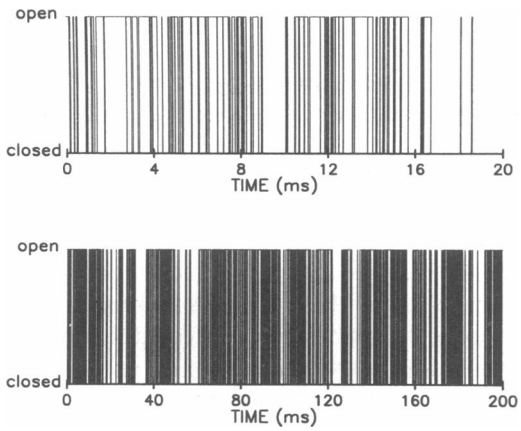

FIGURE 13 Simulated single channel behavior of Model 2. See legend, Fig. 12. Average fraction open = 0.53; 1,053 open-close transitions.

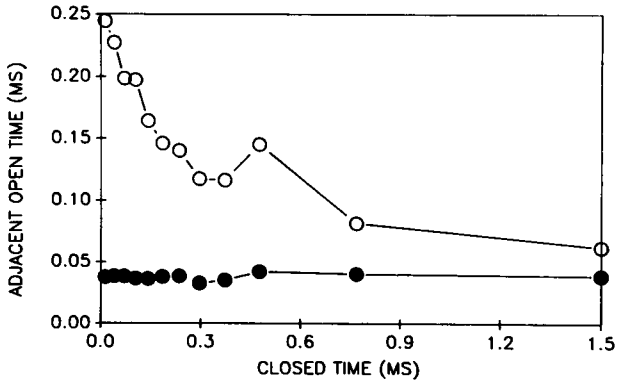

FIGURE 14 Correlation between closed times and adjacent open times for Model 1 (–●–) and Model 2 (–O–). The closed times in a run of 10,000 open-close transitions were grouped into bins and the average value of the adjacent open time determined. The point at 1.5 ms corresponds to the bin for all closed times >1 ms.

open time adjacent to each closed time was determined. Fig. 14 shows the resulting plot for Models 1 and 2. As expected, a strong correlation is apparent for Model 2. No obvious correlation is seen for Model 1. This is consistent with the above conclusion that, for Model 1, the open channel behaves like a single state.

DISCUSSION

Despite the ability of the continuum model to mimic the macroscopic and single channel behavior of experimental channels, it is not likely to usurp the role of the discrete state model as the system of choice for analyzing gating kinetics. The major advantage of the discrete state model is that it has a finite number of adjustable parameters, whereas the continuum model is described by a set of adjustable functions. A number of sophisticated mathematical approaches have been developed for extracting discrete state rate constants from single-channel data (Horn and Lange, 1983; Roux and Sauvé, 1985; Blatz and Magleby, 1986). However, for the case where a large number of closed states are required, the continuum model may offer some advantages in fitting experimental data. For example, White and Bezanilla (1985) used a 16-state model to fit the experimental data for the squid delayed rectifier K^+ channel. They were unable to successfully fit both the conductance and gating current data and suggested their "lack of herculean perseverance" in adjusting the parameters as one explanation. The continuum model discussed here is much simpler. It has only seven adjustable constants (A, B, C, n_g, n_o, D, and k), about the same number as would be required to describe three discrete states.

The major advantage of this continuum model is heuristic. Energy diagrams such as Fig. 2 or 4 provide a simple picture of the global behavior of the channel. From just an analysis of these diagrams, one can predict the major qualitative features of the channel: the delay in channel opening, no delay in channel closing, the time course of the gating current, the bursts of open-close transitions, and the inverse correlation of adjacent open and closed times. In contrast, the behavior of the conventional discrete state model is hidden in the details of the rate constants.

Another advantage of the continuum model is that it may provide a more physically realistic view of the gating process. For example, if the movement of gating charge resulted from rotation and translation of several helical segments (Salkoff et al., 1987), then this analysis predicts the effective rotational diffusion constant of this helix. In the above calculations, a D of 100/s was used to make the results mimic the squid delayed rectifier K^+ channel. This D is in the dimensionless units of the reaction coordinate (x) which varied from 0 to 1. If, instead, a physical X that varied from 0 to L was used, then the corresponding physical diffusion coefficient is equal to D/L^2 (=100/s). Assuming that the helix rotates 60° when x goes from 0 to 1, L becomes equal to $\pi/3$ radians and the rotational diffusion coefficient is equal to ~100/s. To put this value in perspective, the rotational diffusion coefficient of bacteriorhodopsin in a lipid membrane is 8×10^4/s, ~1,000 times larger (Peters and Cherry, 1982). Actually, the charge movement is distributed over four or more helices so that each helix would have to have a diffusion coefficient four times the above estimate. In addition, the rotation of the helices is probably coupled to the conformation of the entire protein. Even with these considerations, the diffusion coefficient which is required to produce the long time delay of the K^+ channel is extremely small, suggesting that there must be a very large "effective" viscosity acting on the conformational movement of the protein. This picture is in agreement with recent analysis that indicates that large conformational changes in proteins can be modeled by continuum frictional forces (McCammon and Harvey, 1987).

APPENDIX

Numerical solution of partial differential equation

The numerical solution is more accurate if the derived functions f_c and f_o are used in place of the functions $C(x)$ and $O(x)$ which describe the probability that the channel is in the closed or open state:

$$f_c(x) = C(x)e^{uc(x)}$$
$$f_o(x) = O(x)e^{uo(x)}. \qquad (1A)$$

Substituting these functions for C and O in Eq. 3, expanding J, and setting $\tau = Dt$,

$$\frac{\partial f_c}{\partial \tau} = \frac{\partial^2 f_c}{\partial x^2} - \frac{duc}{dx}\frac{\partial f_c}{\partial x} + k_o(f_o - f_c)$$
$$\frac{\partial f_o}{\partial \tau} = \frac{\partial^2 f_o}{\partial x^2} - \frac{duo}{dx}\frac{\partial f_o}{\partial x} + k_c(f_c - f_o). \qquad (2A)$$

Boundary condition:

$$\frac{\partial f_c}{\partial x} = \frac{\partial f_o}{\partial x} = 0 \quad \text{at} \quad x = 0 \quad \text{and} \quad x = 1.$$

To obtain the macroscopic rate of channel opening or closing, we assumed the channel to be at equilibrium at the holding voltage v so that the initial conditions for C and O (and f_c and f_o) are given by Eq. 2. Then the voltage is stepped to some new value and the time course of the change in C and O is determined. The equations were solved by using the implicit finite difference approach. (The method was only partially implicit because, e.g., in the f_c equation, the earlier [explicit] value of f_o was used.) The accuracy of the solution was monitored by determining the total (open plus closed) probability (see expression for Q in Eq. 2) at

each time point. If the solution were exact, this probability should be 1 at all times. Any deviation from 1 is a measure of the inaccuracy of the finite difference approximation to the equations or the boundary condition. The spatial and time steps were adjusted so that there was at most a 3% deviation from 1 over the entire time period. The open and closed probabilities were normalized by this total probability at each time point, partially compensating for this error.

Solution for open or closed time frequency distribution

The initial condition for, e.g., the open time frequency, is that $O(x) = 1/h$ for $x = x_o$ and is 0 everywhere else and that $C(x)$ is 0 everywhere (where h is the spatial step size). The system is again described by Eq. 2A, except that k_o is set equal to zero so that the closed state is absorbing.

Gating current calculation

A weighted "center of mass" position of the gating charge is defined by

$$X_g = n_g \int_0^1 [C(x) + O(x)]x\,dx + n_o \int_0^1 O(x)\,dx. \quad (3A)$$

The first term in Eq. 3A is the average x position of the charge n_g that is associated with the reaction coordinate (x). The second term accounts for the charge n_o that is assumed to move through the entire voltage gradient during the close to open transition. At large negative potentials, x_g will approach zero because most of the channels are closed and near $x = 0$; while at large positive potentials, x_g will approach $n_g + n_o$ ($=4$) when most of the channels are open and near $x = 1$. The gating current is equal to the change in X_g divided by the size of the time step.

Single channel simulation

The channel is initially assumed to be open and at $x = x_o$. A time step δ is chosen that is small enough that the probability of an opening or closing transition is <0.1 and the diffusion distance is small. The position of the system after the time step δ is equal to:

$$x(\delta) = x_o + F_r - D\delta \frac{du}{dx}. \quad (4A)$$

The third term on the right is the drift that results from the energy gradient (u is uc or uo, depending on whether the channel is closed or open) and the second term is a random variable chosen from a distribution that has a zero mean and a variance of $2D\delta$. For each time step, the probability of, e.g., a closing, is equal to the probability that a random variable, uniformly distributed on 0 to 1, is less than $k_c(x)\delta$. This is an approximation to the exact exponential distribution, valid for small values of δ.

REFERENCES

Blatz, A. L., and K. L. Magleby. 1986. Correcting single channel data for missed events. *Biophys. J.* 49:967–980.

Cole, K. S., and J. W. Moore. 1960. Potassium ion current in the squid giant axon: dynamic characteristic. *Biophys. J.* 1:1–14.

Colquohoun, D., and B. Sakmann. 1981. Fluctuations in the microsecond time range of the current through single acetylcholine receptor ion channels. *Nature (Lond.).* 294:464–466.

Cooper, K., E. Jakobsson, and P. Wolynes. 1985. The theory of transport through membrane channels. *Prog. Biophys. Mol. Biol.* 46:51–96.

Hille, B. 1984. Ionic Channels of Excitable Membranes. Sinauer Ass., Inc., Sunderland, MA. 337–343.

Hodgkin, A. L., and A. F. Huxley. 1952. A quantitative description of membrane current and its application to conduction and excitation in nerve. *J. Physiol. (Lond.).* 117:500–544.

Horn, R., and K. Lange. 1983. Estimating kinetic constants from single channel data. *Biophys. J.* 43:207–223.

Läuger, P. 1988. Internal motions in proteins and gating kinetics of ionic channels. *Biophys. J.* 53:877–884.

Liebovitch, L. S., and J. M. Sullivan. 1987. Fractal analysis of a voltage-dependent potassium channel from cultured mouse hippocampal neurons. *Biophys. J.* 52:979–988.

McCammon, J. A., and S. C. Harvey. 1987. Dynamics of Proteins and Nucleic Acids. Cambridge University Press, Cambridge, MA. 139–145.

McManus, O. B., A. L. Blatz, and K. L. Magleby. 1985. Inverse relationship of the durations of adjacent open and shut intervals for Cl and K channels. *Nature (Lond.).* 317:625–627.

Millhauser, G. L., E. E. Salpeter, and R. E. Oswald. 1988. Diffusion models of ion-channel gating and the origin of power-law distributions from single channel recording. *Proc. Natl. Acad. Sci. USA.* 85:1503–1507.

Peters, R., and R. Cherry. 1982. Lateral and rotational diffusion of bacteriorhodopsin in lipid bilayers: experimental test of the Saffman-Delbrück equations. *Proc. Natl. Acad. Sci. USA.* 79:4317–4321.

Roux, B., and R. Sauvé. 1985. A general solution to the time interval omission problem applied to single channel analysis. *Biophys. J.* 48:149–158.

Salkoff, L., A. Butler, A. Wei, N. Scavarda, K. Baker, D. Pauron, and C. Smith. 1987. Molecular biology of the voltage-gated sodium channel. *TINS Trends Neurosci.* 10:522–527.

Taylor, R. E., and F. Bezanilla. 1983. Sodium and gating current time shifts resulting from changes in initial conditions. *J. Gen. Physiol.* 81:773–784.

White, M. M., and F. Bezanilla. 1985. Activation of squid axon K^+ channels. Ionic and gating current studies. *J. Gen. Physiol.* 85:539–554.